Lettirei, A., Latour, M., Kauntz Moderini, L., Freddi, F., Rizzano, G. (2022). Design and analysis of damage-free self-centring links for seismic-resilient eccentrically braced frames. The 10th International Conference on the Behaviour of Steel Structures in Seismic Areas, STESSA, Timisoara, Romania, 26–28 May 2022. Lecture Notes in Civil Engineering, vol 262. Springer, Cham. https://doi.org/10.1007/978-3-031-03811-2_82

DESIGN AND ANALYSIS OF DAMAGE-FREE SELF-CENTRING LINKS FOR SEISMIC-RESILIENT ECCENTRICALLY BRACED FRAMES

Annarosa Lettieri[1], Massimo Latour[1], Leo Kauntz Moderini[2], Fabio Freddi[2], Gianvittorio Rizzano[1]

[1] University of Salerno, Italy
[2] University College London, UK
alettieri@unisa.it, mlatour@unisa.it, leo.moderini.18@ucl.ac.uk, f.freddi@ucl.ac.uk, g.rizzano@unisa.it

Abstract. Earthquake resilient steel frames, such as Self-Centring Moment Resisting Frames (SC-MRFs) or Concentrically Braced Frames (SC-CBFs), have been widely studied during the past few years while little attention has been paid to the development of self-centring solutions based on Eccentrically Braced Frames (EBFs). The present paper investigates a possible solution for damage-free self-centring EBFs relying on the use of a damage-free self-centring devices as seismic link. The device uses post-tensioned high-strength steel bars with disks springs to control the self-centring behaviour and friction devices to dissipate seismic energy. A four-storey EBF is designed according to the Eurocode 8 and the third storey of the structure is extracted to investigate the behaviour of a sub-assembly upgraded with the proposed seismic device. A 3D nonlinear finite element model of the device is developed in ABAQUS to evaluate the local behaviour. The results of the conventional and upgraded systems are compared, showing the effectiveness of the solution.

Keywords: Steel Structures, Eccentrically Braced Frames, Damage-Free Self-Centring Links, Structural Resilience, Residual Drifts.

1 Introduction

According to current design codes [1-2], Eccentrically Braced Frames (EBFs), in their traditional configuration, are designed to dissipate the seismic input energy by developing plastic deformations in a segment of the beams denoted as "*seismic link*" or simply "*link*". However, this results in significant economic losses and permanent plastic deformations which could compromise building reparability [3-4]. To overcome these drawbacks, self-centring steel structural systems have been developed over the past decade [5-8]. Only a few research studies focused on the use of EBFs including solutions for residual drifts reductions. Among others, Dubina et al [9] and Ioan et al. [10], investigated a combination of EBFs with removable links and elastic Moment Resisting Frames (MRFs) to reduce or eliminate residual displacements during the reparation process. Cheng et al. [11] investigated a self-centring link beam of EBF in which the rocking interface is located at the interface of the link beam and adjacent beams. Xu et al. [12] presented a self-centring EBF system incorporating post-tensioned high strength steel tendons and super-elastic shape memory alloy bolts. Tong et al. [13] presented the results of an experimental study of D-type self-centring EBF composed of post-tensioned strands and replaceable hysteretic damping devices.

Within this framework, this paper presents a damage-free self-centring link for EBFs, which uses post-tensioned high-strength steel bars (PT-bars) with disk springs to control the self-centring capacity of the frame and friction devices (FDs) to dissipate seismic energy. To investigate the seismic behaviour of this system, finite element (FE) simulations are performed in ABAQUS [14] on a sub-assembly extracted from a four-storey structure designed according to EC8 provisions.

2 Damage free self-centring link

Fig. 1 shows the damage-free self-centring device (SC-link) for EBFs investigated in the present study. It consists of a seismic device placed between the collector beams of an EBF, connected to them through pins. The SC-link is composed of a T-plate and two L-plates connected to the top and bottom flanges of the beams. The damping mechanism of the connection is provided by the longitudinal sliding between the T-plate and L-plates during the rotation of the SC-link. To dissipate the seismic energy, FDs are realised by slotting the web of the T-plate and adding friction pads of thermally sprayed steel shims, pre-stressed with high strength bolts, at the interface of T and L-plates. The slotted holes are designed to accommodate a rotation of 0.08 *rad*, representing the maximum seismic demand assumed by Eurocode 8 for short links under severe seismic events [1]. The self-centring capability is provided by PT-bars placed symmetrically and anchored outside the section of the SC-Link. Besides, disk springs arranged in series and parallel are installed to ensure sufficient deformability to the bars.

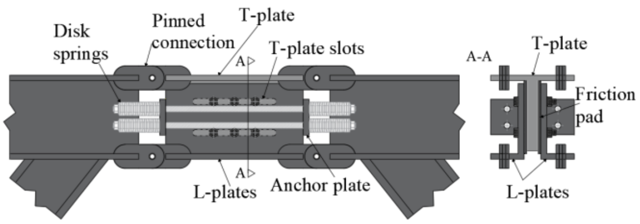

Fig. 1. Concept of the proposed damage-free self-centring link.

Fig. 2(a) shows the forces of the components during the sliding of the SC-link. Fig. 2(b) shows the flag shape cyclic relationship of the SC-link in terms of longitudinal force acting on the link (*i.e.*, F_l), and longitudinal sliding (*i.e.*, δ_l). The force F_0 is the initial post-tensioning of the re-centring system (*i.e.*, $F_{PT,0}$), the longitudinal force F_{FD} represents the sliding forces in the friction pads, while the force ΔF_{PT} is function of the stiffness of the re-centring system (*i.e.*, PT bars and disk springs), and is given by:

$$\Delta F_{PT} = K_{eq}\delta_l \quad (1)$$

where K_{eq} represents the equivalent axial stiffness of the re-centring system defined as:

$$K_{eq} = \frac{K_{PT}K_{ds}}{K_{PT}+K_{ds}}; \qquad K_{PT} = \frac{n_{PT}E_{PT}A_{PT}}{l_{PT}}; \qquad K_{ds} = \frac{n_{ds,par}}{n_{ds,ser}}K_{ds,1}; \quad (2)$$

where n_{PT} is the number of the PT bars employed in the connection, $n_{ds,par}$ and $n_{ds,ser}$ are the number of disk springs arranged in parallel and in series, respectively, and $K_{ds,1}$ is the stiffness of the single disk spring.

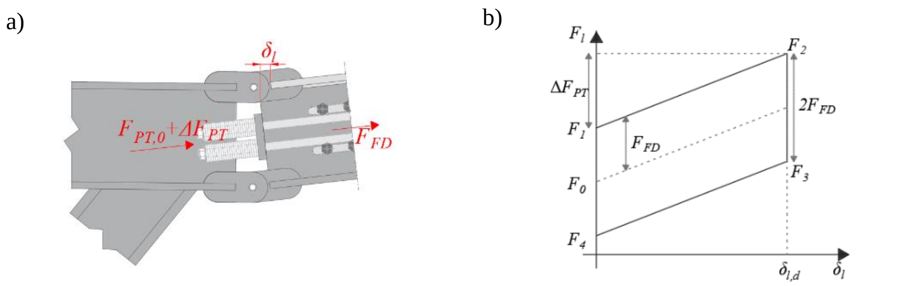

Fig. 2. (a) Forces acting in the self-centring link during rotation; (b) Theoretical longitudinal force-displacement (F_l-δ_l) relationship.

By referring to the F_l-δ_l behaviour, the self-centring capability of the SC-link is achieved if the following relation is satisfied:

$$F_4 \geq 0 \rightarrow F_{PT,0} \geq F_{FD} \quad (3)$$

3 Case-study

A four-storey EBF designed according to EC8 has been considered for case study purposes (see Fig. 3). To preliminarily assess the performance of the proposed SC-link, the third storey of the frame has been extracted, and the cyclic behaviour of such sub-assembly has been assessed considering the conventional configuration and the one upgraded with the SC-link. The Type-1 elastic response spectrum with a peak ground acceleration (PGA) equal to 0.35 g and soil type C has been considered to define the seismic design actions (*i.e.*, Design-Based Earthquake) [1]. The behaviour factor is assumed equal to q = 6.5 according to Eurocode 8 for EBF in DCH [1]. The length *e* of the links is limited at an upper value of 1.6 $M_{p,link}/V_{p,link}$ according to the provisions for short links. Additionally, according to requirements for short links [1], intermediate web stiffeners spaced at an interval not exceeding ($30t_w$ – d/5) are included. Steel S275 is employed for all structural elements (*i.e.*, columns, beams, and braces). The design results are summarised in Table 1. Fig. 4(a) and (b) show the sub-assembly selected in the configuration with the traditional link and with the SC-link, respectively. As suggested by Kasai et al. [15] at the ultimate conditions, corresponding to the maximum value of the rotation between the link and the beam (*i.e.*, θ_P equal to 0.08 *rad* for short links), the bending moments transferred by the columns and bracings of the upper and lower storeys are neglected, hence the static schemes of the sub-assemblies can be assumed hinged at the base. The SC-link has high equal to 280 mm, and it is composed of T and L plates whose geometrical properties are reported in Table 2. As indicated in Fig. 4, the link length in the two configurations is different. In fact, in the traditional EBF, the link length represents the distance between the two ends of the bracings, whereas, in the SC-link, it is the distance between pin connection centres.

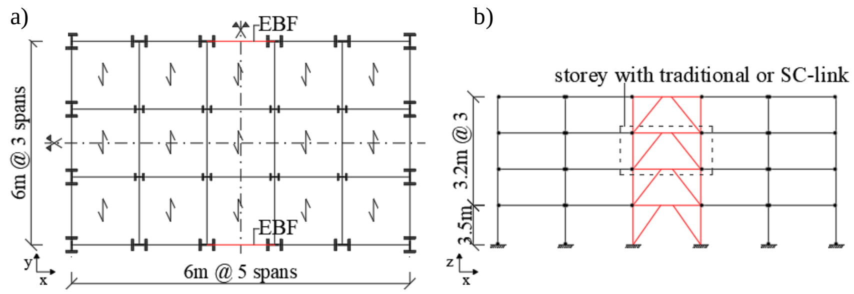

Fig. 3. (a) Plan view of the building; (b) Elevation view of the EBF.

Table 1. Design results for the four-storey EBF.

Storey	Brace section	Column section	Link section	Link length [mm]
1st	HE 220M	HE 320B	HE 360B	1100
2nd	HE 220M	HE 320B	HE 320B	1000
3rd	HE 200M	HE 280B	HE 280B	900
4th	HE 160M	HE 280B	HE 200B	800

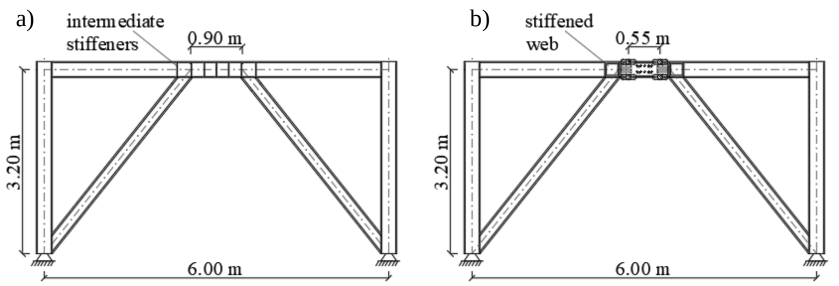

Fig. 4. (a) Static scheme of the case-study with traditional link; (b) Static scheme of the case-study upgraded with SC-link.

Table 2. Geometrical properties of the SC-link.

	h [mm]	t_w [mm]	t_f [mm]	b [mm]	Steel grade
T-plate	126	40	18	280	S275
L-plates	126	20	18	280	S275

4 Design of the damage-free self-centring link

To design each component of the SC-link (*i.e.*, re-centring system and FDs), the longitudinal force acting on the link is derived. In particular, according to the methodology proposed by Kasai et al. [15] the moment equilibrium around a column base point of the free-body diagram of the forces acting on a generic EBF panel (Fig. 5), provides the following relation:

$$F_l = 2\frac{M}{h_d - t_f} = \frac{FHe}{L(h_d - t_f)} \quad (4)$$

where F_l is the longitudinal force of the SC-link, F is the lateral force of the storey, t_f is the flange thickness of the link section.

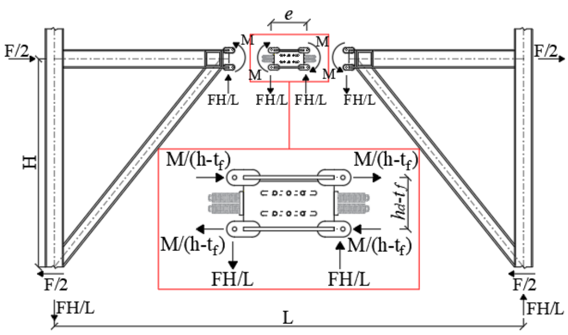

Fig. 5. Free-body diagram of the forces acting on EBF system.

Considering the static scheme reported in Fig. 4(b) subjected to a seismic lateral force of 723 kN, a longitudinal design force (*i.e.*, $F_{l,d}$) equal to 809 kN is derived from Eqn. (5). According to Eqn. (8), in order to provide the self-centring capability of the frame, a force equal to 0.4 $F_{l,d}$ is considered as the action for the design of the FDs, whereas 0.6 $F_{l,d}$ represents the design action for the re-centring system. Successively, the FDs, the PT-bars and the disk springs are designed. The friction pads are chosen according to the results of previous tests carried out by Cavallaro *et al*. [16] and consist of 8 mm of thermally sprayed friction metal steel shims with friction coefficient equal to 0.53 (*i.e.*, μ). Adopting HV M18 10.9 class bolts and a reduction factor ψ equal to 0.4, six bolts are used to develop the required friction force, as derived from Eqn. (5) and considering a sliding force equal to the design action of the FDs. Given the design action of the self-centring system, four M20 threaded bars with a maximum post-tensioning capacity of 156 kN each is adopted to provide the self-centring behaviour. Assuming a maximum rotation of the link equal to 0.08 *rad*, the maximum longitudinal sliding of the SC-link is equal to 24 mm. Finally, disk springs with a resistance of 80 kN and a stiffness equal to 80 kN/mm are adopted.

5 Finite element simulations

Three-dimensional FE models of the case-study frames in both configurations (*i.e.*, EBF with traditional link and with SC-link) are developed in ABAQUS [14]. The models are constituted by *'wire'* elements for column and portions of bracings and beams away from the link, while solid elements are adopted for the other parts (*i.e.*, link section, beams, and bracings close to the link, bolts, bars, anchored plates). A '*tie constraint*' is used to simulate welding among stiffener and beam, bracing and beam, column and beam. The *'surface-to-surface'* interaction property is used to define the contact behaviour among friction interfaces of the FDs. The *'bolt load'* is used to model the pre-loading in the bolts, while post-tensioning in the PT-bars is modelled applying a *'predefined field temperature'*. Cyclic simulations have been performed for the two models considering the same lateral displacement history. Fig. 6(a) and Fig. 7(a) show the results of the simulations for the EBF with traditional link and for EBF with SC-link, respectively. The hysteretic curves of the EBF with traditional link (Fig. 6(a)) have a stable cyclic behaviour characterised by cyclic hardening without degradation of the stiffness. However, the low hardening of the device may induce large residual deformations. Conversely, the results of the EBF with SC-link show that the connection proposed is able to provide the EBF with self-centring capability (Fig. 7(a)) with flag-shaped hysteretic curves similar to the theoretical relationships of Fig. 2(b). Additionally, Von Mises stress distributions are reported in Fig. 6(b) and Fig. 7(b). It can be observed that for the traditional link yielding occurs predominantly in shear, as expected (Fig. 7(a)). Conversely, in all regions of the SC-link are characterised by stresses lower than yielding (Fig. 7(b)).

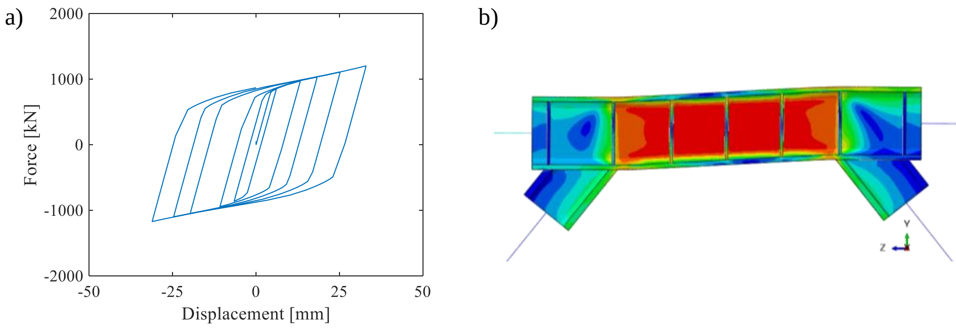

Fig. 6. FE simulation results for EBF with traditional link: (a) hysteretic curves in term of total horizontal force and lateral displacement; (b) Von Mises stresses corresponding to a lateral displacement of 30 mm.

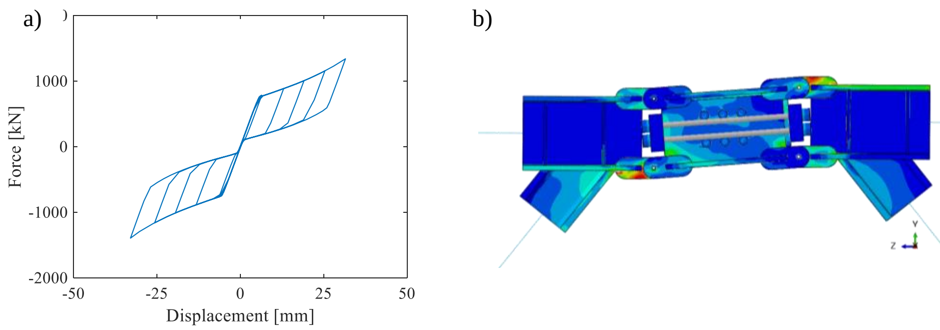

Fig. 7. FE simulation results for EBF with SC-link: (a) hysteretic curves in term of total horizontal force and lateral displacement; (b) Von Mises stresses corresponding to a lateral displacement of 30 mm.

6 Conclusions

The present paper investigates a possible solution for damage-free self-centering EBFs relying on damage-free self-centring devices as seismic links. The device uses post-tensioned high-strength steel bars with disks springs to provide the self-centring behaviour to the link and friction dampers to dissipate the seismic energy. In order to investigate the cyclic behaviour of the connection, a four-storey frame is designed according to Eurocode 8 and the third storey of the structure is extracted and upgraded with the proposed link connection. Both of the configurations (*i.e.*, frame with traditional link and with the damage-free self-centring link) are analysed through three-dimensional finite element modelling carried out in ABAQUS. Cyclic simulations have been performed for the two models applying the same lateral displacement history. The results of the numerical simulations show that the proposed connection is able to restore the frame at the initial configuration providing a flag-shaped hysteretic behaviour.

References

1. EN 1998-1: EUROCODE 8: Design of structures for earthquake resistance – Part 1: General rules, seismic actions and rules for buildings. European Committee for Standardization, Brussels.
2. ASCE/SEI 7-16: Minimum Design Loads and Associated Criteria for Buildings and Other Structures. American Society of Civil Engineers, 2017.
3. Freddi, F., Novelli, V., Gentile, R., Veliu, E., Andonov, A., Andreev, S., Greco, F., Zhuleku, E.: Observations from the 26th November 2019 Albania Earthquake: the Earthquake Engineering Field Investigation Team (EEFIT) mission. Bulletin of Earthquake Engineering 19(5), 2013-2044 (2021).

4. McCormick, J., Aburano, H., Nakashima: Permissible residual deformation levels for building structures considering both safety and human elements. 14th World Conference of Earthquake Engineering, pp. 12-17, China (2008).
5. Latour, M., Rizzano, G., Santiago, A., Da Silva, L.: Experimental response of a low-yielding self-centring, rocking CB joint with friction dampers. Soil Dynamic and Earthquake Engineering 116, 580-592 (2019);
6. Elettore, E., Lettieri, A., Freddi, F., Latour, M., Rizzano, G.: Performance-Based Assessment of Seismic-Resilient Steel Moment Resisting Frames Equipped with Innovative Column Bases Connections. Structures 32: 1646–1664 (2021).
7. Elettore, E., Freddi, F., Latour, M., Rizzano, G.: Design and analysis of a seismic resilient steel moment resisting frame equipped with damage-free self-centering column bases. Journal of Constructional Steel Research 179, (2021).
8. Freddi, F., Dimopoulos, C., Karavasilis, TL.: Experimental evaluation of a rocking damage-free steel column base with friction devices. Journal of Structural Engineering 146(10), (2020).
9. Dubina, D., Stratan, A., Dinu, F.: Dual high-strength steel eccentrically braced frames with removable links. Earthquake Engineering & Structural Dynamics 37, 1703-1720 (2008).
10. Ioan, A., Stratan, A., Dubina, D., Poljansek, M., Molina, FJ., Taucer, P., Pegon, P., Sabau, G.: Experimental validation of re-centring capability of eccentrically braced frames with removable links. Engineering Structures 113, 335-346 (2016).
11. Cheng, CT., Hsu, CH.: Seismic behaviour of self-centering designed eccentrically braced frames. 15th World Conference on Earthquake Engineering, Lisboa (2012).
12. Xu, X., Zhang, Y., Luo, Y.: Self-centering eccentrically braced frames using shape memory alloy bolts and post-tensioned tendons. Journal of Constructional Steel Research 125, 190-204 (2016).
13. Tong, L., Zhang, Y., Zhou, X., Keivan, A., Li, R.: Experimental and Analytical Investigation of D-Type Self-Centering steel eccentrically braced frames with replaceable hysteretic damping devices. Journal of Structural Engineering 145(1), (2019).
14. ABAQUS – Analysis User's Manual Version 6.17, Abaqus Inc., 2017.
15. Kasai, K., Han, X.: New EBF design method and applications: Redesign and analysis of US-Japan EBF. 2nd International Conference on Behaviour of Steel Structures in Seismic Areas (1997).
16. Cavallaro, GF., Francavilla, AB., Latour, M., Piluso, V., Rizzano, G.: Cyclic behaviour of friction materials for low yielding connections. Soil Dynamics and Earthquake Engineering 114, 404-423 (2008).